Pharmaceutical Research, Vol. 24, No. 12, December 2007 (© 2007)
DOI: 10.1007/s11095-007-9367-4

Research Paper

Alginate/Chitosan Nanoparticles are Effective for Oral Insulin Delivery

B. Sarmento,[1,5] A. Ribeiro,[2] F. Veiga,[2] P. Sampaio,[3] R. Neufeld,[4] and D. Ferreira[1]

Received March 13, 2007; accepted June 1, 2007; published online 19 June 2007

Purpose. To evaluate the pharmacological activity of insulin-loaded alginate/chitosan nanoparticles following oral dosage in diabetic rats.
Methods. Nanoparticles were prepared by ionotropic pre-gelation of an alginate core followed by chitosan polyelectrolyte complexation. *In vivo* activity was evaluated by measuring the decrease in blood glucose concentrations in streptozotocin induced, diabetic rats after oral administration and flourescein (FITC)-labelled insulin tracked by confocal microscopy.
Results. Nanoparticles were negatively charged and had a mean size of 750 nm, suitable for uptake within the gastrointestinal tract due to their nanosize range and mucoadhesive properties. The insulin association efficiency was over 70% and insulin was released in a pH-dependent manner under simulated gastrointestinal conditions. Orally delivered nanoparticles lowered basal serum glucose levels by more than 40% with 50 and 100 IU/kg doses sustaining hypoglycemia for over 18 h. Pharmacological availability was 6.8 and 3.4% for the 50 and 100 IU/kg doses respectively, a significant increase over 1.6%, determined for oral insulin alone in solution and over other related studies at the same dose levels. Confocal microscopic examinations of FITC-labelled insulin nanoparticles showed clear adhesion to rat intestinal epithelium, and internalization of insulin within the intestinal mucosa.
Conclusion. The results indicate that the encapsulation of insulin into mucoadhesive nanoparticles was a key factor in the improvement of its oral absorption and oral bioactivity.

KEY WORDS: hypoglycemic effect; insulin; nanoparticle; natural polymers; oral delivery.

INTRODUCTION

Among controlled release formulations, polymeric nano and microparticles have shown interesting promise for protein delivery (1). Nanoparticulate hydrogels consisting of alginate, agar, agarose, chitosan, or synthetic polymers have been developed and tested over the past two decades (2,3). Nanoparticulate delivery systems have the potential to improve protein stability, increase the duration of the therapeutic effect and permit administration through non-parental routes (4).

Oral delivery is the preferred route for administration because it is non-invasive, avoids injections, and decreases risk of infection. It is also physiologically desirable, since the exogenous protein imitates the physiological pathway undergoing first hepatic bypass. The intestinal absorption of proteins has been reported and a combination of mechanisms described to explain how proteins cross the intestinal mucosa. One approach to improve the gastrointestinal uptake of poorly absorbable drugs like insulin is to entrap the protein within colloidal nanoparticles, which provide degradative protection in the gastrointestinal tract and facilitate transport into systemic circulation (2,5). Special attention has been given to mucoadhesive particles which maintain contact with intestinal epithelium for extended periods, promoting penetration of active drug through and between cells due to the concentration gradient between nanoparticles and intestinal membrane. In fact, insulin was observed to be directly internalized by enterocytes in contact with intestine (6,7), and retention of drugs at their absorptive sites by mucoadhesive carriers is a synergic factor. Furthermore, uptake of nanoparticles by the M cells of the Peyer's patches was demonstrated, being absorbed transcellularly, serving as a major gateway for nanoparticle absorption (8–10) as well as absorption through the much more numerous gut enterocytes (11). Endocytosis occurs through clathrin coated pits and vesicles, fluid phase endocytosis and phagocytosis (12). It is well accepted that hydrophobic, negatively charged, protein-loaded nanoparticles smaller that 1 μm potentially show the best absorption rate (13,14), although other factors may govern nanoparticle absorption.

Polymers such as alginate and chitosan have been described as biocompatible, biodegradable and mucoadhesive, enabling numerous pharmaceutical and biomedical applications (15–18) including the design of controlled

[1] Department of Pharmaceutical Technology, Faculty of Pharmacy, University of Porto, Rua Aníbal Cunha 164, 4050-047, Porto, Portugal.
[2] Department of Pharmaceutical Technology, Faculty of Pharmacy, University of Coimbra, Coimbra, Portugal.
[3] Institute of Molecular and Cell Biology, University of Porto, Porto, Portugal.
[4] Chemical Engineering Department, Queen's University, Kingston, Ontario, Canada K7L 3N6.
[5] To whom correspondence should be addressed. (e-mail: bruno.sar mento@ff.up.pt)

release devices. Alginate (Alg) is an anionic polysaccharide of (1–4)-linked β-D-mannuronic acid (M) and α-L-guluronic acid (G) widely used in bioencapsulation of drugs, proteins and cells. The gelling properties of its guluronic residues with divalent ions such as calcium permit the formation of Alg matrices for gels, films, beads, pellets, microparticles and nanoparticles. Chitosan (Chit) is the cationic deacetylated form of chitin [poly-β-(1–4)-*N*-acetyl-D-glucosamine], obtained from exoskeletons of marine arthropods. Chitosan is of interest for a nanoparticulate oral delivery vehicle because it is able to reduce the transepithelial electrical resistance and transiently opening tight conjunction between epithelial cells (19). A variety of Chit-based colloidal delivery vehicles have been described for the association and delivery of drugs (20). We have recently described the nanoencapsulation of insulin in Alg by inducing the ionotropic pre-gelation of a dilute aqueous Alg solution with calcium chloride. Chit then formed a polyelectrolyte complex with alginate (21). Alg/Chit nanoparticles were designed for protection from the aggressive environment of the stomach when administered orally. Insulin was partially retained in a gastric pH environment for up to 24 h while a more extensive release was observed under intestinal pH simulation (21).

Proteins are often unstable and consequently easily damaged during formulation in pharmaceutical dosage forms (22). Insulin-loaded nanoparticles are formulated with organic solvents which are potentially harsh and may denature proteins (23–25). However, ionotropic pre-gelation did not induce conformational changes to the insulin structure in terms of α-helix and β-sheet content (26).

The objectives of the present study were to determine whether the nanoparticulate formulation induced a hypoglycemic effect after oral administration to diabetic rats, and to examine the mechanism of insulin absorption from the GI tract. The rat model was chosen due to its similitude to human and wide acceptance for evaluating the effectiveness of an oral dosage for of insulin, in comparison to other animal models (27–29).

MATERIALS

Low-guluronic content, low viscosity sodium Alg, low molecular weight Chit (≈50 KDa) and calcium chloride were purchased from Sigma (Portugal). Polyanion stock solutions were prepared in deionized water (Milli-Q) overnight under magnetic stirring and Chit samples were dissolved in 1% acetic acid solution in deionized water followed by filtering using a Millipore #2 paper filter and stored at 4°C. Recombinant human crystalline zinc-insulin was a gift from Lilly Portugal. Wistar male rats weighing 200–250 g, were provided by Charles River, Barcelona, Spain. Streptozocin and insulin-flourescein (FITC) from bovine pancreas were from Fluka (Sigma, Portugal). Alexa Fluor 594 conjugate was from Molecular Probes (Oregon, USA). Human insulin detecting ELISA kit (HIEZ 126) was from Linco (Missouri, USA).

Preparation of Nanoparticles

Nanoparticles were prepared from dilute Alg solution containing insulin by inducing an ionotropic pre-gel with calcium counter ions, followed by polyelectrolyte complex coating with Chit, as described previously (21). Particle sizes below 1,000 nm were obtained with 0.05% (w/w) Alg, 0.9 mM of Ca^{2+} and 0.012% (w/w) Chit. The pH of Alg and Chit solutions was adjusted to 4.9 and 4.6, respectively. Nanoparticles were recovered by centrifugation (20,000×*g*/30 min).

Nanoparticle Characterization

Particle size was determined by photon correlation spectroscopy at 25°C with a detection angle of 90° and zeta potential by laser doppler anemometry by using a Malvern Zetasizer and Particle Analyzer 5000 (Malvern Instruments). Measurements were made on aqueous dilute nanoparticle suspension ($n \geq 6$).

The association efficiency (AE) was determined by calculating the difference between the total amount used to prepare the particles and the amount of insulin present in the supernatant after nanoparticle removal by centrifugation. The difference between the total insulin initially used to prepare the particles and the amount of residual unassociated insulin after particle separation as a percent of total nanoparticle dry mass is referred to as loading capacity (LC). Insulin was measured by high-performance liquid chromatography (HPLC).

Insulin *In Vitro* Release from Nanoparticles

Insulin-loaded nanoparticles (200 mg) were placed into 20 ml of HCl buffer at pH 1.2 (USP XXVIII) and incubated at 37°C for 2 h. At determined times, 0.4 ml of supernatant was taken, separated from nanoparticles by centrifugation (20,000×*g*/30 min) for insulin determination and replaced by fresh medium. After 2 h, the nanoparticles were transferred to 20 ml of phosphate buffer at pH 6.8 (USP XXVIII) and incubated at 37°C for an additional 4 h. At determined times, 0.4 ml of supernatant was taken, separated from nanoparticles by centrifugation (20,000×*g*/30 min) for insulin determination and replaced by fresh medium. Release assays were performed in triplicate. Insulin was measured by HPLC.

Insulin Determination

Insulin was determined by HPLC as described in detail previously (30) using a solvent delivery system (Varian 9012)

Table I. Characterization of Alg/Chit Nanoparticles in Terms of Mean Size, Zeta Potential, Insulin AE and LC ($n = 3$, Mean ± SD)

	Size (nm)	Zeta Potential (mV)	AE (%)	LC (%)
Insulin-loaded nanoparticles	748 ± 217	−5.6 ± 1.9	72.8 ± 2.1	9.9 ± 1.5
Unloaded nanoparticles	781 ± 61	−14.5 ± 2.09	–	–

and $\lambda = 214$ nm detector (Varian 9050) equipped with an XTerra RP 18 column, in a gradient method. Time of run was 10 min and eluents were 0.1% trifluoracetic acid aqueous solution and acetonitrile initially set in a 70/30 ratio and linear gradient to 60/40 over 5 min. From 5 to 10 min, ratio was kept constant at 60/40. Final insulin concentrations were calculated with the Varian Star Workstation software against a calibration curve. All measurements were made in triplicate.

In Vivo Pharmacological Activity

Animals were maintained in accordance with the Federation of European Laboratory Animal Science Association and the European Union (Council Directive 86/609/EEC). Male Wistar rats with 250–300 g were housed in cages under controlled temperature and humidity, and fed a laboratory animal standard diet feed (Mucedola Top Certificate, Italy) and provided tap water ad libitum. Lighting was on a 12 h on /12 h off cycle. Rats were rendered diabetic by a single intraperitoneal injection of streptozocin (50 mg/mL in pH 4.5 citrate) at 50 mg/kg. After 2 weeks, rats with fasted blood glucose levels above 250 mg/dL were randomly grouped ($n = 6$) and used for experiments. These rats were fasted 12 h before and 24 h during the experiment, but were allowed water ad libitum. Test samples (1.0 mL) were administered intragastrically by gavage and blood samples (0.2 mL) collected from the tail vein. Sample was separated in two volumes, one to determine plasma glucose level and the other for insulin determination. For insulin determination, serum was separated from the blood samples by centrifugation (5,000 rpm for 10 min) and stored at −80°C until analysis.

Rats were divided into seven groups. Nanoparticles were administered at insulin doses of 25, 50 and 100 IU/kg. Control rats were similarly administered with equivalent volumes of an insulin solution (50 IU/kg), a solution of insulin (50 IU/kg) and empty nanoparticles, or a dispersion of blank nanoparticles. The volume of dispersion and controls administered was 1.0 mL. Also, a control using subcutaneously injected insulin (2.5 IU/kg) was used. Aliquots were collected before and during 24 h period following administration.

Plasma glucose levels were plotted against time to evaluate the cumulative hypoglycemic effect over time after

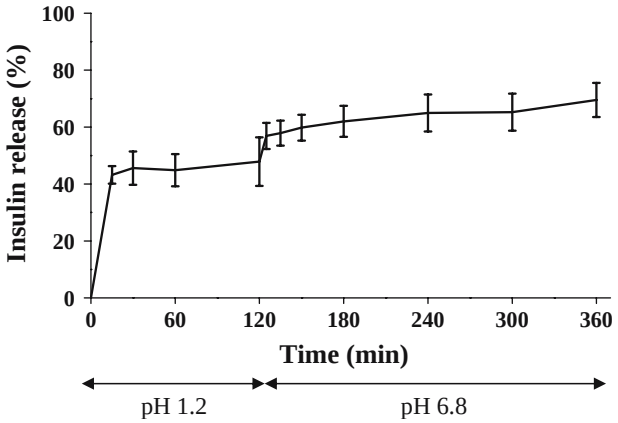

Fig. 1. Insulin release from Alg/Chit nanoparticles produced with Alg/Chit mass ratio of 4.3:1 in gastric pH 1.2 simulated fluid for 120 min followed by 240 min intestinal pH 6.8 simulated fluid at 37°C ($n = 3$, mean ± SD).

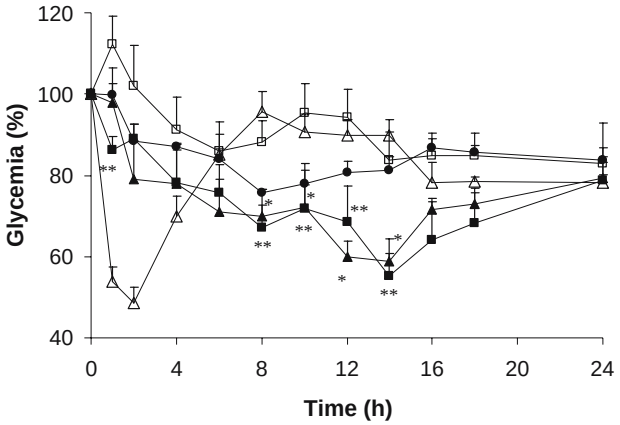

Fig. 2. Plasma glucose levels after administration of insulin-loaded 25 (*black circles*), 50 (*black triangles*) and 100 (*black squares*) IU/kg and empty nanoparticles (*white squares*), compared to 2.5 IU/kg delivered sub-cutaneously (*white triangles*). Data represents the mean ± SEM, $n = 6$ per group. *Single asterisks* 50 IU/kg and *double asterisks* 100 IU/kg dose showed statistically significant differences from negative empty nanoparticle control ($p < 0.05$).

insulin administration, quantified by the area above the curve, determined using the trapezoidal method. Pharmacological availability (PA) of peroral insulin loaded into nanoparticles and in solution were determined as the relative measure of the cumulative reduction in glucose blood levels compared to a 100% availability of the control insulin administered subcutaneously at a dose of 2.5 IU/kg. Plasma insulin levels were plotted against time to evaluate the cumulative amount of insulin delivered to the plasma after insulin administration, quantified by area under the curve.

The cumulative hypoglycemic effect and the cumulative amount of insulin delivered to plasma were calculated for each rat, and a one-way analysis of variance (ANOVA) used to evaluate treatment differences. If the group by each time interaction was significantly different ($p < 0.05$), differences between groups were compared within a post-hoc test (S-N-K). All statistical analyses were performed with the SPSS software package (SPSS for Windows 14.0, SPSS, Chicago, USA).

Plasma glucose level was determined using the Medisense Precision Xceed Kit, (Abbot, Portugal, range 10–600 mg/dL), and expressed as a percent of the baseline plasma glucose level. Serum insulin concentration was measured by a solid two-side enzyme immunoassay (ELISA test kit, Mercodia, Uppsala, Sweden) based on the direct sandwich technique in which two monoclonal antibodies are directed against separate antigenic determinants on the insulin molecule. Serum was separated from blood by centrifugation at 5,000 rpm for 10 min and then 25 μL of sample added to each well of a 96 well microplate using the manufacture's protocol and reading spectroscopically at 450 nm. Results are shown as the mean (±SD) of at least 6 animals.

Tracking FITC-Labelled Nanoparticles

FITC labelled insulin was loaded into nanoparticles to yield 2.0 mg FITC-insulin/mL of nanoparticle suspension and administered by oral gavage to Wistar diabetic rats fasted overnight. The rats were sacrificed 3 h later and intestinal

Table II. Pharmacodynamic Parameters After Oral Administration of Insulin-Loaded Nanoparticles in 25, 50 and 100 IU/kg Doses and Insulin Solution 50 IU/kg

	Hypoglycemic Effect (%)	PA (%)	T_{max} (h)	C_{min} (% basal glucose)
Insulin-loaded nanoparticles (25 IU/kg)	19.9 ± 5.5	7.1 ± 1.7[a]	8	75.7 ± 1.0
Insulin-loaded nanoparticles (50 IU/kg)	27.1 ± 6.7[a]	6.8 ± 1.7[a]	14	58.8 ± 5.4[a]
Insulin-loaded nanoparticles (100 IU/kg)	27.4 ± 8.9[a]	3.4 ± 1.7	14	55.2 ± 5.5[a]
Oral solution (50 IU/kg)	10.8 ± 1.6	1.6 ± 0.7	6	80.8 ± 8.3

Data represents the mean ± SD, $n = 6$ per group

T_{max} = time at minimum relative basal glucose concentration in the blood, C_{min} = minimum relative basal glucose concentration in the blood

[a] Statistically significant differences from oral insulin solution control ($p < 0.05$). Hypoglycemic effect determined based on the area above the curve

segments localized after laparotomy. After washing with isotonic saline, intestine segments were isolated, filled inside with Alexa Fluor 594 solution (0.05% in PBS:glycerol 1:1) and intestinal epithelial cell membranes were stained for 1 h. Tissue was then rinsed, mounted on glass slides and immediately observed using a confocal laser scanning microscope (Leica). Tissue samples were scanned in the x,y plane with a z-step of 500 nm. Since the spectra are not overlapping, FITC-insulin and Alexa Fluor could be analyzed simultaneously with 488 and 561 nm laser respectively. Control rats were dosed with FITC-insulin solution or empty nanoparticles.

RESULTS AND DISCUSSION

Nanoparticles produced by ionotropic pre-gelation of alginate followed by chitosan polyelectrolyte complexation had mean diameter of approximately 750 nm for both insulin-loaded and blank nanoparticles as seen in Table I. Particles with diameters below 1,000 nm are desirable as they are better absorbed in the intestinal tract (11). Zeta potential increased from −14.5 to −5.6 mV with the addition of positively charged insulin, which may partial deposit on the nanoparticle surface. Insulin AE and LC were 72.8 and 9.9% respectively. Previously it was shown that physical properties of Alg/Chit nanoparticles, namely particle size and to a lesser extent AE, were mainly influenced by the Alg/Chit mass ratio (21). Alg/Chit mass ratio of 4.3:1 was selected in the present work with the goal of obtaining a high level of AE and sub-micro particles since additional chitosan mass resulted in increased mean particle size and particle aggregation.

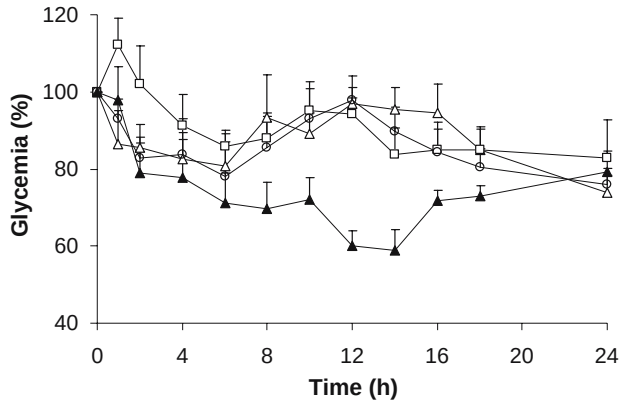

Fig. 3. Plasma glucose levels after oral administration of insulin-loaded nanoparticles 50 IU/kg (*black triangles*), oral insulin solution 50 IU/kg (*white triangles*), empty nanoparticles (*white squares*) and physical mixture of empty nanoparticles and insulin solution 50 IU/kg (*white circles*). Data represents the mean ± SEM, $n = 6$ per group.

The release of insulin from nanoparticles under gastric followed by intestinal simulated pH conditions was investigated. The release profile in Fig. 1 was characterized by an initial rapid release within the first 15 min followed by a plateau state. After 2 h, 45% of the insulin was released. Nanoparticles were then transferred to pH 6.8 buffer simulating intestinal conditions and release was sustained to 70% of the initial amount. The observed immediate release of insulin at pH 1.2 may be related to release from the nanoparticle surface, due to the weak interaction forces between the polyelectrolytes and the protein. However, insulin entrapped within the matrix faced an additional physical barrier. Further gastric protection against insulin release can be attributed to the more effective retention by a tight Alg network that forms at low pH (31,32). At pH 6.8, Alg swells as it forms an ionic state, contributing to a higher amount of insulin release.

The pharmacological effect of insulin loaded nanoparticles was evaluated in diabetic rats dosed orally at loading levels of 25, 50 and 100 IU/kg. Changes in plasma glucose compared to those dosed subcutaneously at 2.5 IU/kg and with empty nanoparticles are shown in Fig. 2. A significant difference in plasma glucose reduction between insulin-loaded and empty nanoparticles was observed, especially 8 to 14 h after administration ($p < 0.05$).

At an insulin dose of 100 IU/kg, a faster onset of action was elicited compared with doses of 25 or 50 IU/kg. The reduction in blood glucose was less in the animals receiving the dose of 25 IU/kg compared with those dosed with 50 and 100 IU/kg. However, the overall plasma glucose levels were similar for doses of 50 and 100 IU/kg. In addition, these higher two dose levels resulted in similar values of cumulative hypoglycemic effect, and similar minimum blood glucose (55% of basal level), as seen in Table II. A dose–response effect was observed between 25 and 50 IU/kg but absent between 50 and 100 IU/kg, which may be due to saturation of the insulin absorption sites at 50 IU/kg. The reduction in blood glucose was less for animals receiving 25 IU/kg, which could indicate that the level of absorption saturation had not been reached. The absence of hypoglycemic effect after administration of empty nanoparticles confirms that the

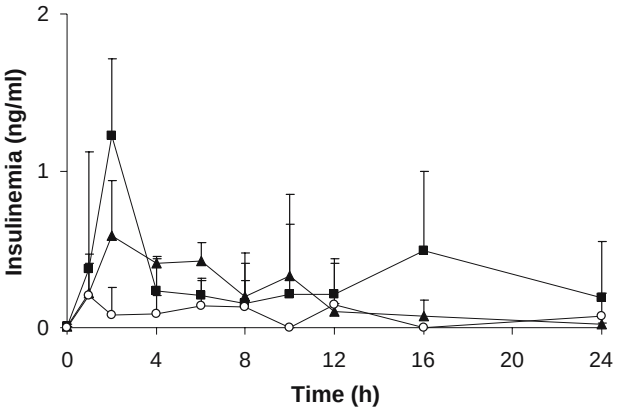

Fig. 4. Serum insulin levels after oral administration of insulin-loaded nanoparticles in 50 (*black triangles*) and 100 (*black squares*) IU/kg doses, and oral insulin solution at 50 IU/kg (*white circles*). Data represents the mean ± SD, $n = 6$ per group.

decrease of blood glucose levels was exclusively due to the physiologic effect of insulin.

To investigate whether nanoparticles enabled intestinal absorption of free insulin, diabetic rats were administered a suspension of empty nanoparticles in insulin solution (50 IU/kg), and comparisons drawn to a group administered insulin solution alone (50 IU/kg). As observed in Fig. 3, both groups showed small hypoglycemic effects between 2 and 8 h after administration. However, this effect appeared sooner and was minor compared to the hypoglycemic effect of the insulin-loaded nanoparticles. A small fraction of the insulin could be absorbed through the intestinal wall exerting a hypoglycaemic effect as observed by others (33,34). In fact, a small amount of human insulin after oral solution administration was detected in the blood by ELISA (Fig. 4), indicating that it was directly absorbed. The direct uptake of insulin has been attributed to specific insulin receptors in intestinal enterocytes (6,7) and rapid internalization by the epithelial cells to the interstitial space from which it reached the blood circulation. The upper intestinal area seems to be the most active region for insulin absorption (35), improved under fasting conditions (36). The observed and prolonged hypoglycemic effect of insulin-loaded nanoparticles compared to the minor effect in animals treated with oral insulin solution leads to the conclusion that Alg/Chit nanoparticles were to some extent able to stabilize and protect entrapped insulin from degradation in the gastrointestinal track. The overall variability of the results obtained was closely similar to other comparable studies (33,34,37) and mainly due to the intrinsic intraspecies variability.

The presence of empty Alg/Chit nanoparticles did not enhance the minor hypoglycemic effect of oral insulin solution, and therefore did not act as insulin absorption enhancer. Only the encapsulation of insulin into nanoparticles and the resulting protective effect enabled nanoparticulate delivery producing a biological response.

It was also observed previously that the physiologic effect of orally dosed insulin encapsulated in Chit mucoadhesive nanoparticles (33,38), and of antitubercular drugs encapsulated in Alg/Chit nanoparticles (39) appeared later than the effect obtained after free drug oral administration. Also, the relative bioavailabilities were significantly higher compared with oral free drug solution, consistent with the results obtained in this study. However, the formulation developed in the present study was able to prolong the hypoglycemic effect of insulin for up to 24 h compared with nanoparticles exclusively composed by Chit where the hypoglycemic effect was observed for less than 12 h (38) or in lower extent (33). The presence of a core material composed of counter-charged Alg, complexed with a shell material of chitosan, may improve nanoparticle stability better retaining insulin within the nanoparticle matrix. Thus, the presence of an Alg core might explain the improved physiologic effect by increasing two-fold the PA from 4% obtained for Chit nanoparticles (33) to 7% found in the present work.

Serum insulin levels following intragastric administration of insulin-loaded nanoparticles are shown in Fig. 4, and pharmacokinetic parameters summarized in Table III. Increasing serum insulin levels were observed during the first 2 h following by lower continuous levels for 12 and 16 h with doses of 50 and 100 IU/kg, respectively. The initial insulin peak is probably related with the free insulin initially released from nanoparticles, directly absorbed and then eliminated from the blood by physiologic excretion. Then subsequent continuous absorption resulting in a stable level may be explained by continuous arrival of nanoparticles at the absorptive sites, and sustained release of insulin from the nanoparticles. Temporary retention of the mucoadhesive nanoparticles in the upper intestine and late arrival to the preferred sites for insulin absorption (35) and for nanoparticle uptake in the posterior ileum (13,40) may contribute to the delayed prolonged insulinemia values. Adhering nanoparticles remain at the insulin uptake sites for longer than that of released insulin, and thus continue to release insulin in a sustained manner. In addition, the extent of

Table III. Pharmacokinetic Parameters for Serum Insulin Levels After Oral Administration of Insulin-Loaded Nanoparticles in Both 50 and 100 IU/kg Doses and Insulin Solution 50 IU/kg

	Bioavailability (ng/mL h)	T_{max} (h)	C_{max} (ng/mL)
Insulin-loaded nanoparticles (50 IU/kg)	5.1 ± 2.1[a]	2	0.59 ± 0.30
Insulin-loaded nanoparticles (100 IU/kg)	9.5 ± 3.7[a]	2	1.66 ± 0.86
Oral Insulin solution (50 IU/kg)	2.1 ± 0.9	1	0.20 ± 0.10

Data represents the mean ± SD, $n = 6$ per group
T_{max} = time at maximum concentration of insulin in the blood, C_{max} = maximum concentration of insulin in the blood
[a] Statistically significant differences from oral insulin solution control ($p < 0.05$). Bioavailability determined based on area under the curve

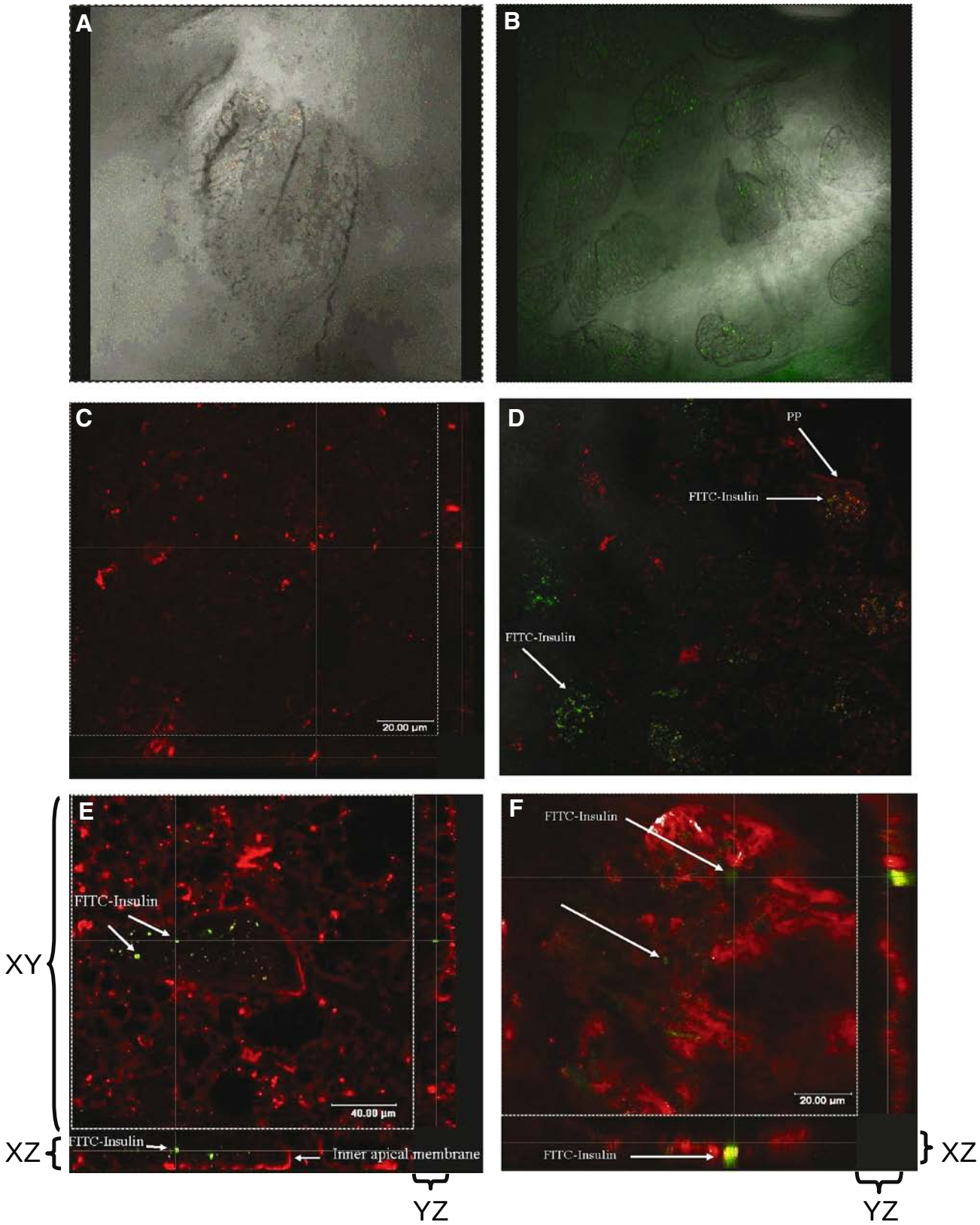

Fig. 5. Confocal scanning microscopy images showing the association of FITC-insulin (*green*) to intestinal tissue (cell membranes in *red*). **A** Control intestinal section showing the villi. **B** Inner apical intestinal section of rat treated with FITC-insulin oral solution. **C** Intestinal section of rat treated with empty nanoparticles and Alexa Fluor colorant. **D** Inner apical intestinal section of rat with Peyer's patches (*PP*) treated with FITC-insulin nanoparticles. Peyer's area show a deep green fluorescence. **E** Inner apical intestinal section of Peyer's patch areas of rat treated with FITC-insulin nanoparticles. **F** Inner apical upper intestinal section of rat treated with FITC-insulin nanoparticles. The three-dimensional plan shows the internalization of labelled insulin. *Grey lines* indicate the plans were pictures were analyzed.

release within the gastrointestinal track may be much less than observed *in vitro* due to the viscous lumen and fasted animal conditions.

The removal of insulin from the site of absorption may be considered to be one of the barriers against free insulin absorption. For this reason, increasing the retention time on the mucosa due to adhesive particles can improve bioavailability (41,42), which is concluded from Table III. It is also possible that uptake of nanoparticles by Peyer's patches in the posterior ileum (2) can contribute to the maintenance of insulinemia and consequent hypoglycaemic effect.

In general, bioavailability for reported oral insulin trials has been low. For instance, pH-responsive poly(methacrylic-*g*-ethylene glycol) hydrogel microparticles as oral insulin delivery systems to diabetic rats resulted in bioavailability less than 2.5% (37) and chitosan nanoparticles resulted in bioavailability around 4% (33). Even for the new oral insulin formulations under clinical evaluation, the bioavailability is still limited (43). However, the bioavailability of 7% obtained in the present work is considerably higher than that of previous studies showing improved insulin absorption.

The mechanism and location of insulin absorption was examined using FITC-insulin. Figure 5 shows confocal images of intestinal sections after oral nanoparticle administration. Fluorescence was observed throughout the ileum tissue, both on the surface of the intestinal enterocytes and on the M-cells. As suggested above, the retention of insulin on the mucosa due to nanoparticle mucoadhesion and further insulin absorption appears to be demonstrated by the presence of FITC-insulin on the apical membrane of the intestine 3 h after administration. Also the dense Peyer's patches region of the posterior ileum appeared labelled as seen in Fig. 5D. Interaction of nanoparticles with M-cells of the Peyer's patches would suggest that nanoparticles were concentrated on the follicle associate epithelium promoting the absorption of the insulin. Peyer's patches have previously been associated with nanoparticle uptake (2,5,44), occurring through adsorptive endocytosis (45). The location of the fluorescent insulin may be seen below the surface layer of the enterocytes inside the intestinal wall in the three-dimensional section of Fig. 5E, F (lateral X–Z plan) suggesting that the insulin is at various stages of internalization in the ileum. In the negative control of rats treated with empty nanoparticles, autofluoresce associated with the intestinal tissue was not observed (Fig. 5C). After oral administration of FITC-insulin solution, slight green fluorescence is visible associated with the intestinal walls and its mucus, even after rinsing with isotonic solution (Fig. 5B), possibly due to residual fluorescent products attached to the mucus associated with the intestinal walls.

No one mechanism appears dominant in insulin uptake. Besides providing protection from degradation in the gastrointestinal tract, the mucoadhesive (46) and absorption-enhancing properties of Chit (19,47,48) and Alg (49) may contribute to the high insulin concentration on the surface of the intestinal wall and to its diffusion through the epithelium, promoting insulin absorption. Furthermore, Chit is able to reversibly alter tight junctions without provoking damage to the cell membrane and without affecting the viability of intestinal epithelial cells (33,50). Mucoadhesive nanoparticles penetrating the mucous layer are able to prolong the residence time and the insulin released can interact deeply and permeate the intestinal barrier to the bloodstream. Simultaneously, paracellular absorption and endocytosis may be considered as synergic mechanisms for insulin absorption (2). The paracellular pathway has been observed to contribute to protein absorption since it has been shown that most protein and polypeptide drugs diffuse through the aqueous-filled tight junctional pathway due to their hydrophilic nature (51). However, it is commonly identified as limiting the absorption rate, due to the low surface area and tightness of the junctions of the intercellular spaces (51). Internalization of insulin via adsorptive endocytosis occurring by non-specific interactions of nanoparticles with the cell membrane (52) or through clathrin mediated interactions (53) has been demonstrated as valid mechanisms for insulin absorption. Also, the direct uptake of nanoparticles carrying proteins by enterocytes is a limited but potential process, as recently reviewed (2), contributing to the total amount of absorbed insulin. Furthermore, the uptake of the nanoparticles by the M cells overlaying the Peyer's patches can contribute to a longer hypoglycaemic response (33,54).

CONCLUSION

Insulin-loaded alginate/chitosan nanoparticles produced by ionotropic pre-gelation/polyelectrolyte complexation, provided markedly enhanced intestinal absorption of insulin following oral administration. Nanoparticles lowered serum glucose levels of streptozotocin-induced diabetic rats at insulin doses of 50 and 100 IU/kg up to 59 and 55% respectively, of their basal glucose level. The hypoglycemic effect and insulinemia levels were significantly higher than that obtained from oral insulin solution and physical mixture of oral insulin and empty nanoparticles, revealing two to four fold improvement of oral relative PA. In addition, the physiological effect was observed for more than 18 h. The mechanism of insulin absorption seems to be a combination of both insulin internalization, probably through vesicular structures in enterocytes and insulin-loaded nanoparticle uptake by Peyer patches. Alginate/chitosan nanoparticles appear promising as an oral delivery system for insulin and potentially for other therapeutical proteins.

ACKNOWLEDGEMENTS

This work was supported by Fundação para a Ciência e Tecnologia, Portugal and by the Natural Sciences and Engineering Research Council of Canada. The authors wish to thank Lilly Portugal for insulin supply.

REFERENCES

1. F. Delie and M. J. Blanco-Prieto. Polymeric particulates to improve oral bioavailability of peptide drugs *Molecules* **10**:65–80 (2005).
2. A. des Rieux, V. Fievez, M. Garinot, Y.-J. Schneider, and V. Preat. Nanoparticles as potential oral delivery systems of proteins and vaccines: A mechanistic approach *J. Control. Release* **116**:1–27 (2006).

3. S. A. Galindo-Rodriguez, E. Allémann, H. Fassi, and E. Doelker. Polymeric nanoparticles for oral delivery of drugs and vacines: A critical evaluation of *in vivo* studies *Crit. Rev. Ther. Drug* **22**:419–463 (2005).
4. A. Florence. The oral absorption of micro- and nanoparticulates: Neither exceptional nor unusual *Pharm. Res.* **14**:259–266 (1997).
5. M. Morishita and N. A. Peppas. Is the oral route possible for peptide and protein drug delivery? *Drug Discov. Today* **11**:905–910 (2006).
6. M. Bendayan, E. Ziv, D. Gingras, R. Ben-Sasson, H. Bar-On, and M. Kidron. Biochemical and morpho-cytochemical evidence for the intestinal absorption of insulin in control and diabetic rats. Comparison between the effectiveness of duodenal and colon mucosa *Diabetologia* **37**:119–126 (1994).
7. E. Ziv and M. Bendayan. Intestinal absorption of peptides through the enterocytes *Microsc. Res. Tech.* **49**:346–352 (2000).
8. A. Fasano. Innovative strategies for the oral delivery of drugs and peptides *Trends Biotechnol.* **16**:152–157 (1998).
9. H. Pinto-Alphandary, M. Aboubakar, D. Jaillard, P. Couvreur, and C. Vauthier. Visualization of insulin-loaded nanocapsules: *in vitro* and *in vivo* studies after oral administration to rats *Pharm. Res.* **20**:1071–1084 (2003).
10. O. Borges, A. Cordeiro-da-Silva, S. G. Romeijn, M. Amidi, A. de Sousa, G. Borchard, and H. E. Junginger. Uptake studies in rat Peyer's patches, cytotoxicity and release studies of alginate coated chitosan nanoparticles for mucosal vaccination *J. Control. Release* **114**:348–358 (2006).
11. N. Hussain, V. Jaitley, and A. T. Florence. Recent advances in the understanding of uptake of microparticulates across the gastrointestinal lymphatics *Adv. Drug Deliv. Rev.* **50**:107–142 (2001).
12. M. G. Qaddoumi, H. J. Gukasyan, J. Davda, V. Labhasetwar, K. J. Kim, and V. H. Lee. Clathrin and caveolin-1 expression in primary pigmented rabbit conjunctival epithelial cells: role in PLGA nanoparticle endocytosis *Mol. Vis.* **9**:559–568 (2003).
13. T. Jung, W. Kamm, A. Breitenbach, E. Kaiserling, J. X. Xiao, and T. Kissel. Biodegradable nanoparticles for oral delivery of peptides: is there a role for polymers to affect mucosal uptake? *Eur. J. Pharm. Biopharm.* **50**:147–160 (2000).
14. H. S. Yoo and T. G. Park. Biodegradable nanoparticles containing protein–fatty acid complexes for oral delivery of salmon calcitonin *J. Pharm. Sci.* **93**:488–495 (2004).
15. W. Tiyaboonchai, J. Woiszwillo, R. C. Sims, and C. R. Middaugh. Insulin containing polyethylenimine-dextran sulfate nanoparticles *Int. J. Pharm.* **255**:139–151 (2003).
16. W. R. Gombotz and S. F. Wee. Protein release from alginate matrices *Adv. Drug Deliv. Rev.* **31**:267–285 (1998).
17. L. Ilium. Chitosan and its use as a pharmaceutical excipient *Pharm. Res.* **15**:1326–1331 (1998).
18. L. Illum, N. F. Farraj, and S. S. Davis. Chitosan as a novel nasal delivery system for peptide drugs *Pharm. Res.* **11**:1186–1189 (1994).
19. P. Artursson. Effect of chitosan on the permeability of monolayers of intestinal epithelial cells (Caco-2) *Pharm. Res.* **11**:1358–1361 (1994).
20. M. Prabaharan and J. F. Mano. Chitosan-based particles as controlled drug delivery systems *Drug Deliv.* **12**:41–57 (2005).
21. B. Sarmento, A. J. Ribeiro, F. Veiga, D. C. Ferreira, and R. J. Neufeld. Insulin-loaded nanoparticles are prepared by alginate ionotropic pre-gelation followed by chitosan polyelectrolyte complexation. *J. Nanosci. Nanotechnol.* **7**:2833–2841 (2007).
22. M. van de Weert, W. E. Hennink, and W. Jiskoot. Protein instability in poly(lactic-co-glycolic acid) microparticles *Pharm. Res.* **17**:1159–1167 (2000).
23. C. Damge, H. Vrancks, P. Balschmidt, and P. Couvreur. Poly(alkyl cyanoacrylate) nanospheres for oral administration of insulin *J. Pharm. Sci.* **86**:1407–1500 (1997).
24. G. P. Carino, J. S. Jacob, and E. Mathiowitz. Nanosphere based oral insulin delivery *J. Control. Release* **65**:261–269 (2000).
25. X. Y. Ma, G. M. Pan, Z. Lu, J. S. Hu, J. Z. Bei, J. H. Jia, and S. G. Wang. Preliminary study of oral polylactide microcapsulated insulin *in vitro* and *in vivo Diabetes Obes. Metab.* **2**:243–250 (2000).
26. B. Sarmento, D. C. Ferreira, L. Jorgensen, and M. van de Weert. Probing insulin's secondary structure after entrapment into alginate/chitosan nanoparticles *Eur. J. Pharm. Biopharm.* **65**:10–17 (2007).
27. T. K. Tugrul. Comparison of the gastrointestinal anatomy, physiology, and biochemistry of humans and commonly used laboratory animals *Biopharm. Drug Dispos.* **16**:351–380 (1995).
28. X. Cao, S. Gibbs, L. Fang, H. Miller, C. Landowski, H.-C. Shin, H. Lennernas, Y. Zhong, G. Amidon, L. Yu, and D. Sun. Why is it challenging to predict intestinal drug absorption and oral bioavailability in human using rat model *Pharm. Res.* **23**:1675–1686 (2006).
29. M. M. Lerco, C. T. Spadella, and J. L. M. Machado. Experimental alloxan diabetes-induced: a model for clinical and laboratory studies in rats *Acta Cir. Bras.* **18**:132–142 (2003).
30. B. Sarmento, A. Ribeiro, F. Veiga, and D. Ferreira. Development and validation of a rapid reversed-phase HPLC method for the determination of insulin from nanoparticulate systems *Biomed. Chromatogr.* **20**:898–903 (2006).
31. G. Coppi, V. Iannuccelli, E. Leo, M. T. Bernabei, and R. Cameroni. Protein immobilization in crosslinked alginate microparticles *J. Microencapsul.* **19**:37–44 (2002).
32. G. W. Vandenberg and J. De La Noue. Evaluation of protein release from chitosan-alginate microcapsules produced using external or internal gelation *J. Microencapsul.* **18**:433–441 (2001).
33. Z. Ma, T. M. Lim, and L.-Y. Lim. Pharmacological activity of peroral chitosan-insulin nanoparticles in diabetic rats *Int. J. Pharm.* **293**:271–280 (2005).
34. Y. Pan, Y. J. Li, H. Y. Zhao, J. M. Zheng, H. Xu, G. Wei, J. S. Hao, and F. D. Cui. Bioadhesive polysaccharide in protein delivery system: chitosan nanoparticles improve the intestinal absorption of insulin *in vivo Int. J. Pharm.* **249**:139–147 (2002).
35. M. Morishita, I. Morishita, K. Takayama, Y. Machida, and T. Nagai. Site-dependent effect of aprotinin, sodium caprate, Na2EDTA and sodium glycocholate on intestinal absorption of insulin *Biol. Pharm. Bull.* **16**:68–72 (1993).
36. N. Gallo-Payet and J. S. Hugon. Insulin receptors in isolated adult mouse intestinal cells: studies *in vivo* and in organ culture *Endocrinology* **114**:1885–1892 (1984).
37. A. M. Lowman, M. Morishita, M. Kajita, T. Nagai, and N. A. Peppas. Oral delivery of insulin using pH-responsive complexation gels *J. Pharm. Sci.* **88**:933–937 (1999).
38. Y. H. Lin, F. L. Mi, C. T. Chen, W. C. Chang, S. F. Peng, H. F. Liang, and H. W. Sung. Preparation and characterization of nanoparticles shelled with chitosan for oral insulin delivery *Biomacromolecules* **8**:146–152 (2007).
39. Z. Ahmad, R. Pandey, S. Sharma, and G. K. Khuller. Pharmacokinetic and pharmacodynamic behaviour of antitubercular drugs encapsulated in alginate nanoparticles at two doses *Int. J. Antimicrob. Agents* **27**:409–416 (2006).
40. F. Cui, K. Shi, L. Zhang, A. Tao, and Y. Kawashima. Biodegradable nanoparticles loaded with insulin–phospholipid complex for oral delivery: Preparation, *in vitro* characterization and *in vivo* evaluation *J. Control. Release* **114**:242–250 (2006).
41. J. Kreuter. *Colloidal drug delivery systems*, M. Dekker, New York, 1994.
42. P. Couvreur, C. Dubernet, and F. Puisieux. Controlled drug delivery with nanoparticles: current possibilities and future trends *Eur. J. Pharm. Biopharm.* **41**:2–13 (1995).
43. A. Amin, T. Shah, J. Patel, and A. Gajjar. Current status of non-invasive insulin delivery technologies *Drug Deliv. Technol.* **7**:48–55 (2007).
44. H. Chen and R. Langer. Oral particulate delivery: status and future trends *Adv. Drug Deliv. Rev.* **34**:339–350 (1998).
45. A. Buda, C. Sands, and M. A. Jepson. Use of fluorescence imaging to investigate the structure and function of intestinal M cells *Adv. Drug Deliv. Rev.* **57**:123–134 (2005).
46. C.-M. Lehr, J. A. Bouwstra, E. H. Schacht, and H. E. Junginger. *In vitro* evaluation of mucoadhesive properties of chitosan and some other natural polymers *Int. J. Pharm.* **78**:43–48 (1992).
47. K. A. Janes, P. Calvo, and M. J. Alonso. Polysaccharide colloidal particles as delivery systems for macromolecules *Adv. Drug Deliv. Rev.* **47**:83–97 (2001).

48. L. Illum. Chitosan and its use as a pharmaceutical excipient *Pharm. Res.* **15**:1326–1331 (1998).
49. M. George and T. E. Abraham. Polyionic hydrocolloids for the intestinal delivery of protein drugs: Alginate and chitosan—a review *J. Control. Release* **114**:1–14 (2006).
50. M. Thanou, J. C. Verhoef, and H. E. Junginger. Chitosan and its derivatives as intestinal absorption enhancers *Adv. Drug Deliv. Rev.* **50**:91–101 (2001).
51. N. Salamat-Miller and T. P. Johnston. Current strategies used to enhance the paracellular transport of therapeutic polypeptides across the intestinal epithelium *Int. J. Pharm.* **294**:201–216 (2005).
52. S. Mao, O. Germershaus, D. Fischer, T. Linn, R. Schnepf, and T. Kissel. Uptake and transport of PEG-graft-trimethyl-chitosan copolymers as insulin nanocomplexes by epithelial cells *Pharm. Res.* **22**:2058–2068 (2005).
53. Z. Ma and L.-Y. Lim. Uptake of chitosan and associated insulin in Caco-2 cell monolayers: a comparison between chitosan molecules and chitosan nanoparticles *Pharm. Res.* **20**:1812–1819 (2003).
54. C. Prego, D. Torres, and M. J. Alonso. The potential of chitosan for the oral administration of peptides *Expert. Opin. Drug Deliv.* **2**:843–854 (2005).